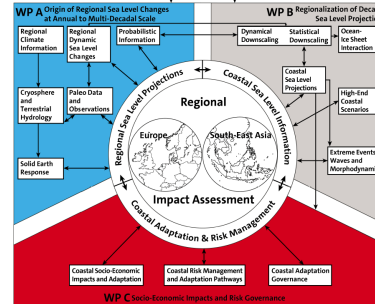




Highlights Ocean 2017-2018

AG Oceanography, Uni Bremen



RACE!
REGIONAL ATLANTIC CIRCULATION AND GLOBAL CHANGE



How well is the North Atlantic circulation simulated in models?

Tilia Breckenfelder, Monika Rhein, Achim Roessler and Christian Mertens

The North Atlantic Current (NAC) transports warm and saline water from the subtropical Atlantic to the high latitudes, and thereby significantly influences the climate and sea level in western and northern Europe. Despite its importance, continuous observations of the strength of that circulation are only available on some locations, and none of those time series is longer than 25 years. This is much too short to analyse variability on multiannual to decadal time scales and their linkage to the atmosphere and climate. These topics have to be studied with models, but for that they need to simulate a realistic circulation.

To find out whether this is the case, observed transport time series in the subpolar North Atlantic are compared with the modelled circulation (Breckenfelder et al., 2017), and this was a joint effort of the observational group at the IUP and the model group of C. Böning at GEOMAR, Kiel.

The simulated NAC transport across the Mid-Atlantic Ridge from the western into the eastern Atlantic (27 Sv) was only slightly lower than observed, but the NAC pathways were shifted further northward. In the eastern Atlantic, the western branch of the NAC carries the bulk of the transport, while episodic observations point to a preference of the eastern branch. In short, the model is able to simulate the

main features of the flow, giving confidence to analyse multiannual and their linkages to

atmospheric modes in the model. It turned out that the modelled NAC transports were significantly larger during high NAO phases (+6.7 Sv) by mainly enhancing the transport of the eastern NAC branch.

This research is part of the BMBF funded program **RACE** (Regional Atlantic Circulation and Global Change).

Reference:

Breckenfelder, T., M. Rhein, A. Roessler, C. W. Böning, A. Biastoch, E. Behrens, and C. Mertens: Flow paths and variability of the North Atlantic Current: A comparison of observations and a high-resolution model. *J. Geophys. Res.*, 122, 2686-2708, doi:10.1002/2016JC012444, 2017.

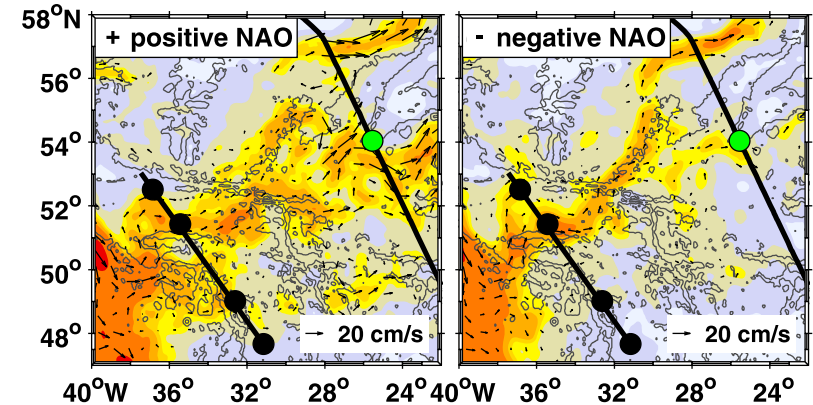


Figure 63: Modelled integrated flow field, 0-1000m depth for time periods with high positive NAO (left) and high negative NAO (right). From Breckenfelder et al., 2017

Where is the Greenland melt water?

Monika Rhein, Reiner Steinfeldt, Oliver Huhn and Tilia Breckenfelder

Global warming will lead to significant changes in the Atlantic circulation, with enormous impact on the European climate and the sea level in Europe and North America in the next decades. However, the projected changes in the circulation are still uncertain. When we continue to burn fossil fuels as we do now, the AMOC is thought to decline till 2100 by 10 % to 50 %, depending on the climate model. One open question is the response of the large-scale Atlantic circulation to increasing Greenland melt. Greenland's mass loss has quadrupled over the last two decades, by surface melt and by contact of the warm water of subtropical origin with glaciers terminating in the ocean fjords. When the additional freshwater invades the central Labrador Sea that links the northward subtropical warm water with the southward transport of cold water in the abyss, then this link could be weakened or interrupted leading to a decline in the northward warm water transport. While in typical climate models the Greenland melt water reaches the key region quickly, it takes much longer in a high resolution ocean-ice model, where most of the freshwater first sticks to the Greenland boundary current and only part makes it into the central Labrador Sea.

What about observations? In the presence of various freshwater sources and saline water masses, salinity measurements alone are not sufficient to identify Greenland melt, and other parameters are needed. The noble gases helium and neon are trapped in air bubbles in the ice, and when ice

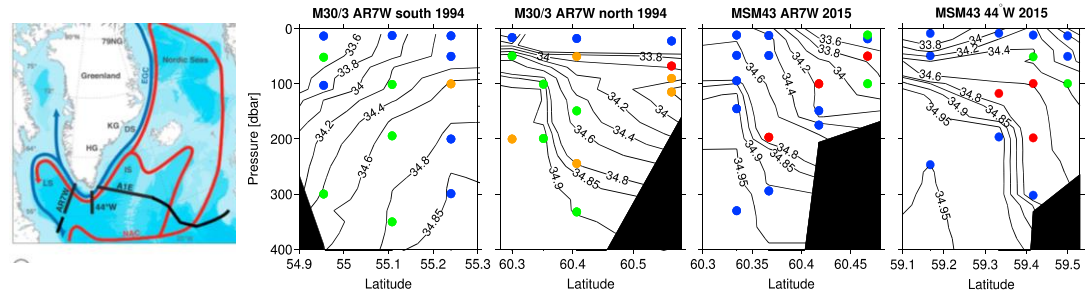


Figure 64: Distribution of SMW fraction (%) in the upper 400 m at the Greenland and Canadian Shelf (location see map). Blue: SMW not detected, dark red: >0.23%, green between 0.075% and 0.2%. From Rhein et al., 2018.

melts below the mixed layer, these noble gases are dissolved in ocean water. By measuring the distribution of He and Ne, fractions of submarine Greenland meltwater (SMW) down to less than 1 per mill are identified. We used this method for the first time to quantify the distribution of Greenland melt. SMW fractions >0.2% (maximum 0.62%) are confined in the upper 400 m of the Greenland and Canadian boundary current, but is not detectable in the central Labrador Sea yet. Occasionally, He and Ne signals are also found in the deep water masses, but they enter the abyss by a different process. We hypothesize that SMW bearing water leaves the Greenland shelf in the northern Irminger Sea with the so-called East Greenland Current spill jets.

This research is part of the BMBF funded program **RACE** (Regional Atlantic Circulation and Global Change) and of the DFG funded priority program **SPP 1889** Regional Sea Level and Society

Reference:

Rhein, M., Steinfeldt, R., Huhn, O., Sültenfuss, J., and Breckenfelder, T.: Greenland submarine melt water observed in the Labrador and Irminger Sea. *Geophysical Research Letters*, 45, 10,570–10,578. <https://doi.org/10.1029/2018GL079110>, 2018.

Internal waves generated by remote tropical cyclones

Janna Köhler, Georg S. Völker and Maren Walter

Internal waves radiate energy and momentum horizontally and vertically through the interior of the ocean, thereby changing the density field as they distort (i.e. vertically displace) the background density interfaces. These vertical displacements can reach up to some hundred meters, depending on the internal wave energy and the local stratification whereas horizontal scales of internal waves range in the order of 100 –1000m. They span the frequency range from the local Coriolis frequency f to the buoyancy frequency N that is set by the stratification (Figure 65). Internal waves have a variety of energy sources and generation processes. Major generation mechanisms are e.g. the interaction of the barotropic tides with the seafloor topography inducing internal waves with tidal frequencies or large scale currents interacting with the seafloor topography. A fluctuating wind stress at the ocean surface induces downward propagating low frequency, near inertial (near the Coriolis frequency f) internal waves. This can induce a seasonal cycle in near-inertial internal wave energy that is largely in phase with storm intensity. Once the internal waves are generated, they undergo a multitude of propagation and interaction processes which induce a propagation of energy towards smaller scales until the internal waves finally break and cause diapycnal mixing and energy dissipation.

To address the question of how far hurricane-generated near-inertial waves propagate before their energy is dissipated, we studied the temporal variability of near-inertial internal wave energy south of the main hurricane track. For this we used a 5-yr mooring time series in the interior of the tropical North Atlantic at 16°N. The distinctly calm oceanographic and meteorological conditions in the mooring area are characterized by weak and constant trade winds. This allows the clear identification of near-inertial waves that were

remotely generated by hurricanes and propagate southward towards the mooring area.

During all deployment periods, hurricanes passed over or to the North of the mooring, with the strongest winds occurring in 2003 and 2004 (Figure 66). In the 2003 hurricane season, two very strong hurricanes (Isabel and Fabian) passed over the tropical Atlantic within several days of each other (Figure 67 panel a). With a time lag of approximately 2 to 3 weeks after the passage of the two hurricanes, an increase in depth-mean near-inertial energy by a factor of 3.8 is observed in the mooring area (Figure 67 panel b). Weaker hurricanes in 2001, 2002, and 2004 correspond to smaller increases in energy (factors of 1.1, 1.8, and 2.4 times the background, respectively). It was shown that near-inertial waves with frequencies corresponding to generation sites of up to approximately 1000 km north of the mooring contribute to the amplifications in 2003 and 2004 (Figure 67 panel c).

The energy flux measured at the mooring location during the strongest hurricanes in 2003, shows a matching strong (up to 5 kW m^{-1}) southward energy flux from mid-September to mid-

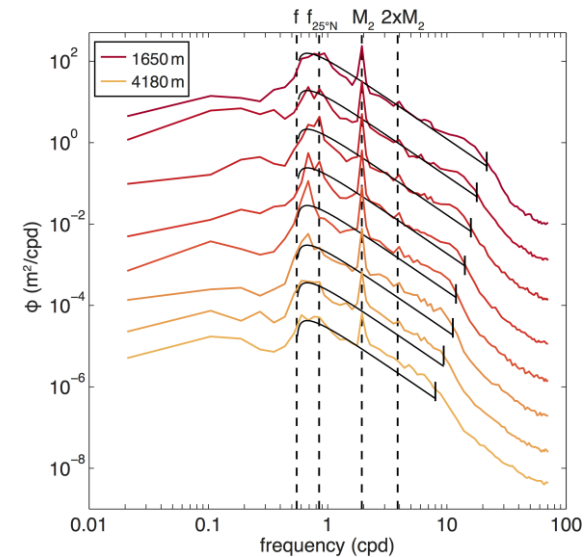


Figure 65: Mean spectra of vertical displacements of isopycnals during the fourth deployment period with corresponding Garrett Munk spectra (black). Vertical black dashed lines denote the inertial frequency at the mooring site (f), at 25°N ($f_{25^\circ N}$), the M_2 tidal frequency, and $2M_2$, respectively. The small vertical black bars show the buoyancy frequency at the individual depths. Spectra have been vertically offset by 10^{-1} for clarity (with zero offset for the uppermost instrument).

October 2003. During the rest of the year, only a weak flux lacking a dominant direction is observed, making the hurricane-induced energy flux the dominating contribution to the time-integrated horizontal energy flux over the entire year. In the zonal flux component, individual flux estimates are enhanced during September and October, but as no direction prevails, the time-integrated en-

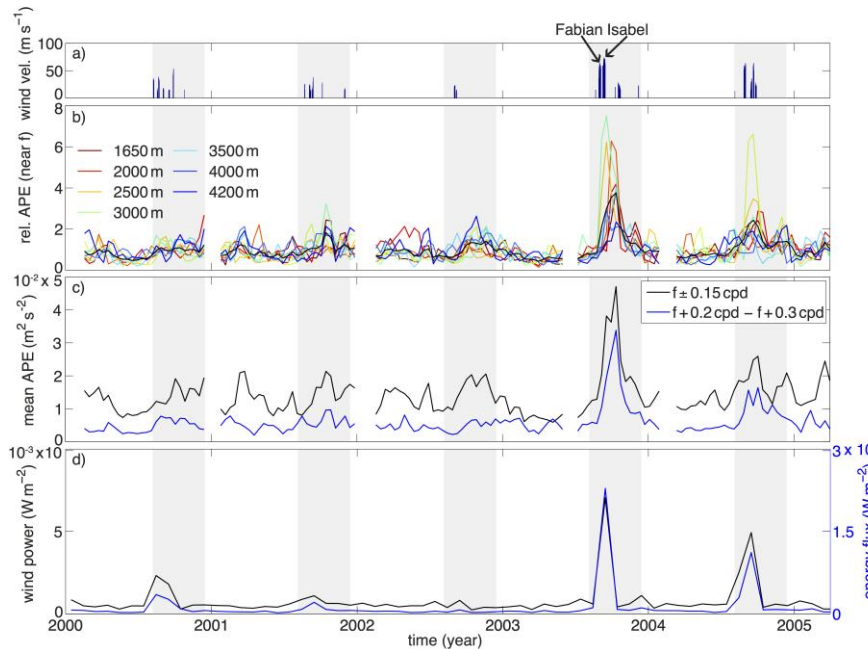


Figure 67: Wind speeds of hurricanes at times when they pass the area $15^{\circ}\text{N} < \text{lat} < 25^{\circ}\text{N}$ and $45^{\circ}\text{W} < \text{lon} < 70^{\circ}\text{W}$ (data from HURDAT2). (b) Time series of near-inertial ($f - 0.15$ to $f + 0.3$ cpd) energy divided by its mean over the entire 5 years at the individual depths along with the mean (over depth) value (black). (c) Mean (over depth) of potential energy in the frequency ranges $f \pm 0.15$ cpd (black) and $f + 0.2$ to $f + 0.3$ cpd (blue). (d) Energy flux (normalized by area) from the wind field into the mixed layer (blue) and into the internal wave field (black) from the extended slab model in the area $15^{\circ}\text{--}25^{\circ}\text{N}$, $45^{\circ}\text{--}70^{\circ}\text{W}$.

ergy flux is much lower than in the meridional component (approx. 1×10^9 to $5 \times 10^9 \text{ J m}^{-1}$).

For a qualitative comparison, the energy imparted to the internal gravity wave field by the wind was estimated using an extended slab model. With the exception of hurricanes, the wind-induced inertial energy flux into the internal wave field has little variability around an average value below $4 \times 10^{-5} \text{ W m}^{-2}$ (Figure 67 panel d). Compared to other regions, this is relatively small and reflects the generally calm weather regime at the mooring location. Superimposed on these background conditions are sporadic peaks (up to at least 5 times higher than background) in the energy fluxes into the internal gravity wave field, which can be linked to the strong winds of passing hurricanes. These peaks precede observed increases in the APE at the mooring location by approximately 1 month. This also suggests that the internal gravity waves associated with the increase in APE are not generated on site, but at some distance, and propagate toward the mooring location.

These results show that hurricanes centred up to several hundred kilometres north of the mooring are the dominant energy source of near-inertial waves in the central part of the western tropical Atlantic and thus contribute to the energy available for diapycnal mixing in regions far to the South of the storm track.

References

Köhler, J., G. S. Völker, and M. Walter: Response of the internal wave field to remote wind forcing by tropical cyclones. *J. Phys. Oceanogr.*, 48(2), 317-328, 2018.

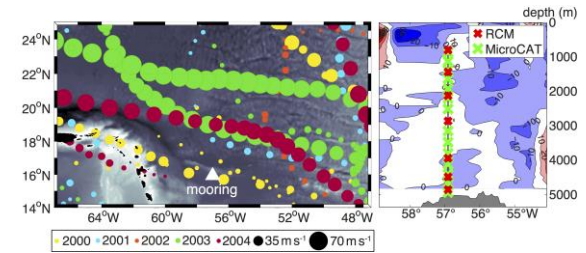


Figure 66: Location of the central mooring of the MOVE array along with hurricane tracks (from the Atlantic hurricane database, HURDAT2) during 2000-2004 (left). Distribution of temperature and conductivity sensors and current meters (RCMs) shown as an example for the deployment period 2003-04 with current measurements from a cruise in June 2000 in the background (right).

Basal melt and freezing rates from first noble gas samples beneath an ice shelf

Oliver Huhn, Monika Rhein and Jürgen Sültenfuß

In austral summer 2015/16 and 2016/17 we obtained with a new constructed gas-tight in-situ water sampler the worldwide first noble-gas samples from below an ice shelf, the Filchner Ice Shelf in the southern Weddell Sea, Antarctica (Huhn et al., 2018).

Quantifying the amount of glacial meltwater (GMW) that is released from the large floating ice shelves surrounding Antarctica into the ocean is crucial to understand the complex ocean-ice shelf interaction under warming climate conditions. Direct observations of basal melt rates are rare, due to the remote and hardly accessible areas. The Filchner-Ronne Ice Shelf (FRIS) is the largest by volume in Antarctica, and models suggest an accelerated basal melting to the end of this century. However, actual estimates of its basal melt rate are usually based on indirect methods, i.e. model simulations and remote sensing techniques.

The stable noble gases helium and neon are useful tracers to quantify GMW. They are weakly soluble in seawater, and therefore are present in low concentrations. But glacial ice traps atmospheric air. When the meteoric ice melts at the base of an ice shelf, the enhanced hydrostatic

pressure at several hundred meter depth causes the trapped noble gasses to dissolve fully in the water. This leads to a He excess of 1280% and a Ne excess of 890% in pure GMW. This large excess provides an excellent tool to detect and quantify GMW fractions as low as 0.05%.

To quantify the fraction and the spatial distribution of GMW below the Filchner Ice Shelf (FIS), we collected the first sub-ice shelf helium and neon samples from six boreholes (Figure 68) located on FIS, hot-water drilled by a team from the British Antarctic Survey (BAS) and the Alfred-Wegener-Institute (AWI) in the framework of the "Filchner Ice Shelf Project" (FISP) and the "Filchner Ice Shelf System" (FISS).

To obtain noble gas samples from the water column below an ice shelf, we have constructed a new gas-tight in-situ water sampler. The major challenge was to protect the water samples from the sub-glacial cavity from gas-fractionation and degassing due to freezing and expansion while the sample is recovered through the

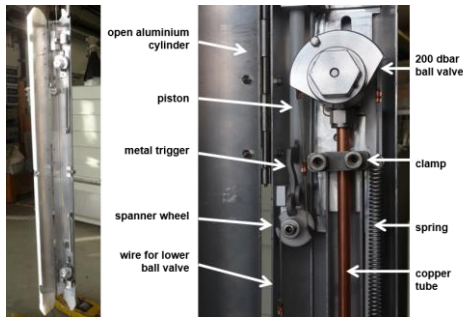


Figure 69: In-situ sub-ice-shelf water sampler. Left: photo of the entire in-situ water sampler in the machine shop. Right: details of the upper closing mechanism inside the in-situ water sampler showing release piston, metal trigger, spanner wheel, spring, and valve with connected copper tube.

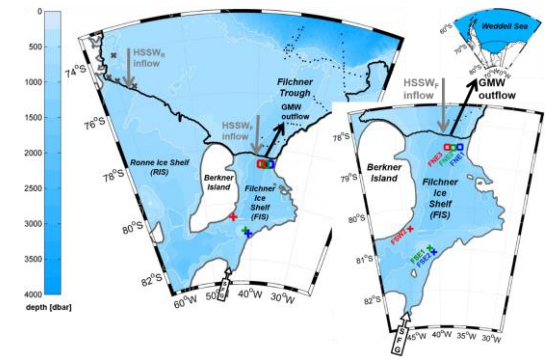


Figure 68: Map of the FRIS showing ice drill sites with noble gas data. Bold black line: ice shelf front, thick grey line: approximate grounding line. Blue shading: isobaths in 250 m steps, thin white lines: 500 m and 1000 m isobaths. Berkner Island separates Ronne Ice Shelf (RIS) to the west from FIS. In the southeast, Support Force Glacier (SFG) drains into FIS. Red, green, and blue crosses are the locations of the southern sites with noble gas data from 2015/16. Red, green, and blue squares are the northern sites from 2016/17. Black dots north of FIS are noble gas stations from 2014, grey crosses in front of RIS are noble gas stations from 1995. Grey and black arrows indicate the inflow of High Salinity Shelf Water (HSSW, subscript F and R denoting FIS and RIS inflow) and the outflow of glacial meltwater (GMW).

air-filled portion of the up to 800 m long and 25 cm narrow bore-hole at -20°C.

The instrument (Figure 69) contains a copper tube allowing a sea-water sample of ~44 g to be collected, with high pressure ball valves connected to a gas-tight connector at both ends. Additional inflow and outflow funnels extend the tube at both ends of the sampling device to increase the flux of water for flushing and rinsing the copper tube. The instrument is mounted in an aluminium

cylinder (diameter 10 cm, length 150 cm, weight 8 kg) to protect it while passing through the bore hole.

The instrument is lowered into the ice shelf cavity on a wire together with a CTD profiler continuously measuring temperature, salinity and pressure. During lowering the valves are held open with a steel spring and connecting wires. A messenger weight deployed along the wire then strikes a piston, releasing a spanner wheel held back by a metal trigger arm and closing the valves at each end of the sample tube.

Three sites at around

81°S between Berkner Island and the mainland were occupied in 2015/16, and are representative of the part of the ice shelf cavity, where inflow from the Ronne Ice Shelf (RIS) in the west determines the water column structure. Three sites around 78.5°S were sampled in 2016/17. They are located ~60 km south of the FIS ice front and could potentially be influenced by water masses formed north of the ice shelf. The FIS cavity samples are supplemented by oceanic noble gas samples in front of FIS and RIS to determine the properties of inflowing and outflowing water.

Basal meltwater fractions (Figure 70B) calculated from helium and neon (Figure 70A) range from 3.6% near the ice shelf base to 0.5% near the sea floor, with distinct regional differences. We estimate an average basal melt rate for the FRIS of 177 ± 95 Gt/year, independently confirming previous results. We calculate that up to 2.7% of the meltwater has been refrozen. Furthermore, we identified a local source of crustal ^4He (at the south-eastern-most location, fed by Support Forth Glacier), that contributes up to 13 % subglacial runoff (accumulated α -particles from the underlying bedrock into the overlaying ice stream before the glacier starts floating) to the total meltwater.

Our results provide a benchmark against which ice shelf cavity conditions in models investigating the interaction between the ocean and ice shelves can be compared.

Reference:

Huhn, O., T. Hattermann, P. E. D. Davis, E. Dunker, H. H. Hellmer, K. W. Nicholls, S. Østerhus, M. Rhein, M. Schröder, J. Sültenfuß: Basal melt and freezing rates from first noble gas samples beneath an ice shelf. *Geophysical Research Letters*, 45, doi:10.1029/2018GL079706, 2018.

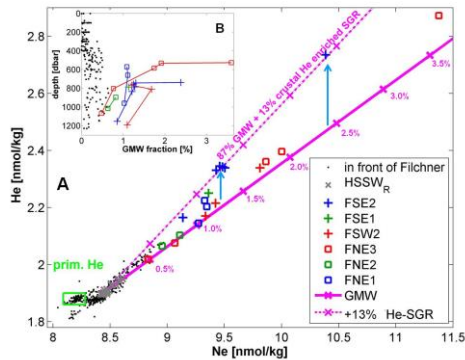


Figure 70 (A) Ne vs. He and (B) calculated GMW fractions below FIS and in front of FIS. Data colours and symbols as in the map above. A) shows the correlation between He and Ne. Solid magenta line indicates mixing of inflowing High Salinity Shelf Water into the RIS cavity and pure GMW (Ne +890 ‰; He +1280 ‰). The magenta marks on the GMW line indicate GMW fraction every 0.5%. He concentrations above the GMW mixing line indicate addition of crustal He accumulated in the ice from α -decay from the underlying bedrock. The dashed magenta line represents mixing between HSSW and a combination of 87% GMW plus 13% crustal He enriched subglacial runoff (SGR). B) shows the calculated GMW fractions based on Ne.

Temperature flux carried by individual eddies across 47°N in the Atlantic Ocean

Vasco Müller, Dagmar Kieke and Christian Mertens

The North Atlantic between 40°–55°N is influenced by two vastly different regimes of currents and water masses: the subpolar gyre, a large-scale cyclonic circulation cell, and the anticyclonic circulation cell of the subtropical gyre. In the Newfoundland Basin, the Western Boundary Current (WBC) and the North Atlantic Current (NAC), the northward continuation of the Gulf Stream, flow in different directions along the boundary of the two gyres. The deep reaching WBC originating in the north transports cold and fresh water of subpolar origin southward. The NAC, on the other hand, carries warmer and saline surface and subsurface waters of subtropical origin into the North Atlantic.

In a recent study (Müller et al., 2017) done in collaboration with scientists from the University of Alberta, Edmonton, Canada, we investigated the western subpolar North Atlantic between 45°N and 50°N, which is a highly dynamic region. On its way along the western continental margin, the Gulf Stream/NAC has to cross several topographic obstacles causing it to experience disruptions, forming meanders, and shedding individual eddies, i.e. small whirling bodies of water rotating either in clockwise or anti-clockwise direction. This creates regions of increased eddy kinetic energy (EKE) along the pathway of the NAC and in the Newfoundland Basin (Figure 71).

Over a period spanning about two decades, we identified, tracked, and analyzed these eddies while crossing the latitude of 47°N. The purpose of our study was to contribute to a better understanding of the role of individual eddies for

the spatial exchange of waters and heat and horizontal mixing of water masses from different origin and of

properties. We centred our analysis on surface temperature fluxes of individual eddies, detected in satellite altimetry and sea surface temperature (SST) observations based on an algorithm provided by Nencioli et al. (2010). Both data sets have the advantage of high temporal and spatial coverage and thus provide a long-term time series spanning over more than two decades (1993–2014) at a high temporal and spatial resolution (1 day and 1/4°). As a comparison, the analysis was subsequently applied to the output from two Canadian model simulations with different horizontal resolution (1/4° and 1/12°).

For the eddy detection and the calculation of the respective temperature fluxes, the two independent data sets (observations and the model simulations) all showed coherent patterns. The highest numbers of eddies in the subpolar North Atlantic were detected along the pathway of the NAC and in the observations also on the Grand Banks of Newfoundland. Furthermore, the study illustrated the importance of individual eddies, carrying a notably large tem-

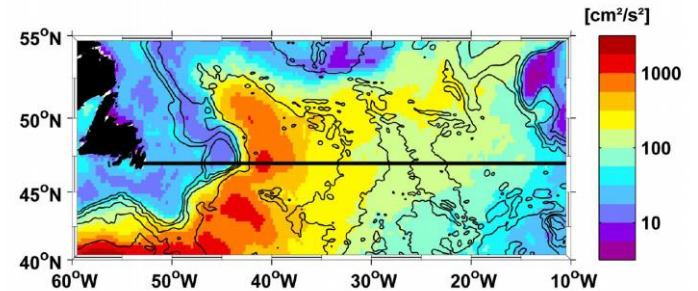


Figure 71: Mean eddy kinetic energy (EKE) relative to the annual cycle derived from geostrophic surface velocity anomalies of the years 1993 to 2014. EKE [cm^2/s^2] is shown with a logarithmic scale. Highest EKE values are typically found along the pathway of the North Atlantic Current (NAC). The black bold line denotes the 47°N section.

perature anomaly (so-called strong eddies), for the temperature flux by eddies across 47°N. About 25% of the absolute temperature flux by eddies crossing 47°N originated from these strong eddies. Strong eddies occurred most often in the Newfoundland Basin. The number of both strong and regular eddies in the region and their respective direction of translation was clearly connected to the spatial pattern and strength of the background oceanic velocity field (Figure 72). The western part of the Newfoundland Basin with the fastest and most pronounced current branches was the major pathway for eddies and their associated temperature flux across 47°N. Among the investigated eddies northward moving cold-core cyclones carrying subpolar water from the WBC made a considerable contribution to the overall temperature flux by eddies in the Newfoundland Basin.

Even though we found the largest temperature fluxes in either direction in the western boundary region, the mean flux in the western basin was practically zero, because the large northward flux (especially in the NAC region) was compensated by large southward fluxes in the Newfoundland Basin Recirculation (NBR) region around 40°W and in the WBC. The eddies, first detected in the region between WBC and NAC, provided a means for the local exchange between the boundary and the interior of the North Atlantic. Contrary to the western basin, the eastern basin of the North Atlantic showed a rather low temperature flux carried by eddies across 47°N, the main reason being the NAC running mainly in a zonal direction northward of the section.

This study was carried out in the framework of the German-Canadian international research training group *ArcTrain*, funded by the German Research Foundation (DFG).

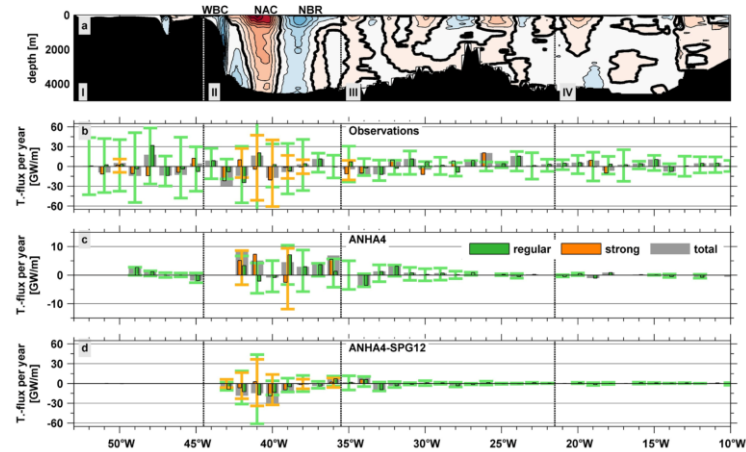


Figure 72: (a) Meridional background velocity from the observations and the (b) sum of the temperature flux by eddies per 1° bin along 47°N (normalized by the number of years) in the observations (January 1993 to April 2014), (c) 1/4° ANHA4 simulation (2002 to 2013), and (d) 1/12° ANHA4-SPG12 simulation (2002 to 2013). The net flux (grey) is separated into fluxes carried by regular (green) and by strong (orange) eddies. Vertical bars show the sum of the temperature flux by eddies of regular (green) and strong (orange) eddies in either direction. The vertical whiskers represent the standard deviation of the respective flux in either direction. NAC: North Atlantic Current; NBR: Newfoundland Basin Recirculation.

References:

- Müller, V., D. Kieke, P. G. Myers, C. Pennelly, and C. Mertens: Temperature flux carried by individual eddies across 47°N in the Atlantic Ocean, *J. Geophys. Res.*, 122, 2441-2464, doi:10.1002/2016JC012175, 2017.
- Nencioli, F., C. Dong, T. Dickey, L. Washburn, and J. C. McWilliams: A vector geometry-based eddy detection algorithm and its application to a high-resolution numerical model product and high-frequency radar surface velocities in the Southern California Bight, *J. Atmos. Oceanic Technol.*, 27(3), 564–579, doi:10.1175/2009JTECHO725.1, 2010.